DOI : 10.5958/0974-0112.2018.00005.1

Indian J. Hort. 75(1), March 2018: 27-33

Acreage estimation of mango orchards using hyperspectral satellite data

Nobin C. Paul, Prachi M. Sahoo*, Tauqueer Ahmad, R.N. Sahoo*, Gopal Krishna and S.B. Lal****

Division of Sample Surveys, ICAR-Indian Agricultural Statistics Research Institute, Library Avenue, New Delhi 110012

ABSTRACT

Horticultural crop plays a unique role in India's economy, therefore reliable and timely estimates of area under horticulture crops are of vital importance. Present methods of crop acreage estimation rely heavily on sample survey approach which is time consuming for a diversified and large country like India. Modern space technology with advance tools of Remote Sensing, GIS and GPS may be an alternative option for estimating area under horticultural crops. The advantage of using satellite data is that it provides both synoptic view and the economies of scale, since data over large areas could be gathered quickly from such platforms. This study has been undertaken to estimate the acreage under mango and to map existing orchards of Mango using hyperspectral satellite data. The study was conducted for Meerut district of Uttar Pradesh. The hyperion hyperspectral satellite data was evaluated to estimate the area under all mango orchards. These estimates were compared with actual area under mango orchards measured using Global Positioning System (GPS) and the total area under mango was predicted as 961.88 ha which was 92% close to ground data 889.65 ha. The results indicated the scope of hyperspectral remote sensing in acreage estimation of fruit crops.

Key words: Endmember extraction, ground control point, root mean square error, spectral angle mapper.

INTRODUCTION

Horticultural crops play a significant role in economy, health, food and self-reliance of any country. During past few years, horticulture development has emerged as one of the major thrust area in agriculture sector. Horticultural crops play a unique role in India's economy and nutritional security. It contributes more than 33% to GDP of agriculture (Economic Survey, 2015-16) and among horticultural crops India has been placed at 2nd position in the world for production of fruits and vegetables. The fruit crops solely share 32.19% of total production of major horticultural crops of the country. For optimum utilization of available horticultural land resources on a sustainable basis, timely and reliable information regarding their nature, spatial extent is important which means accurate discrimination of horticultural crops is necessary for giving area under the crop which acts as a vital input for taking valuable decision regarding planning, policy making and exports at national level. Till date usually sample survey techniques are applied for estimating area and production of horticultural crops, which is time consuming, involves lot of field survey and less accurate. With the advancement in space technology and the emergence of modern tools like remote sensing and Geographic Information System it may be easier, quicker and faster to estimate area under horticultural crops which has been explored in the present study.Most of the studies on crop acreage estimation using satellite image also involves the use of multispectral data like Landsat TM (7 bands), LISS II (4 bands), LISS III (4 bands), SPOT 5 (4 bands), MODIS (36 bands) faced difficulties in crop identification. Major limitation of multispectral data is lesser number of bands and mixed pixels which may not be able to discriminate fruit crops. Because of lesser number of bands in multispectral data, it gives a discrete spectrum, which fails to identify minute differences in reflectance pattern of different crops particularly fruit crops. Hyperspectral data has relatively large number of narrow, contiguous bands which lead to continuous spectral reflectance curve, making intricate details visible in the spectrum. There are some research work related to acreage estimation of fruit crops which includes: Gordon and Phillipson (3) first explored the usefulness of Landsat TM sensor data for estimating area of fruit trees in New York State. TM satellite data shows promise in distinguishing fruit trees but the main problem which was encountered was mixing of forests and fruit trees signatures made it difficult to separate forests from fruit trees. Due to low spatial resolution, the orchard rows were not discriminated from the forest.Yadav *et al.* (6) initiated a study to estimate the acreage and production of mango orchards using IRS LISS-II and LISS-III sensor data. They found difficulty in identification of mango orchards due to the mixing

*Corresponding author's E-mail: prachi.iasri@gmail.com
**Cabin, ICAR-IASRI, Library Avenue, Pusa, New Delhi, 110012
***Div. of Agril. Physics, ICAR-IARI, New Delhi 110012

of different varieties, variation in the age of the fruit trees, mixing of the signature with other plantation crops like coconut, sapota, mixing of signatures of young plantations of mango with that of vegetation.

According to the results, mango acreage estimation using satellite data leads to deviation of 6.32% (LISS-II) and 12.71% (LISS-III) from the actual estimates as released by Department of Horticulture, Government of India. Nagaraja (4) made an attempt to estimate acreage of mango growing areas using IRS 1C LISS-III (23.5 and 70.5 m) and MODIS (250 m., 500 m. and 1000 m.) data for Saharanpur district of Uttar Pradesh. Unsupervised, supervised, decision tree and spectral angle mapping techniques were used for classification and acreage estimation of mango. The study clearly shows the usefulness of IRS 1C LISS-III data for identifying mango orchards and acreage estimation. Decision tree approach was found to be more reliable. Presently estimates of area of fruit crops are obtained through labour-intensive methods using multispectral satellite data, which are less precise and does not give in-depth information about different species. Schupp *et al*. (9) stated that future improvements in orchard production and associated equipment may be done using laser, videos and satellite imaging technologies. Many studies has endorsed the potential of hyperspectral imagery for area estimation, fruit yield estimation and plant stress identification (Tajeda *et al.*, 10; Ye *et al.*, 11) So far, not much work on acreage estimation of fruit crops using hyperspectral satellite data has been attempted. Therefore, this study has been taken with an objective of acreage estimation of mango orchards using hyperspectral satellite data of Meerut district, Uttar Pradesh.

MATERIALS AND METHODS

Part of Meerut district of Uttar Pradesh corresponding to coverage of hyperspectral sensor, Hyperion of EO-1 satellite was consideredfor area estimation of fruit crops. However, ground survey done later confirmed Mango as only dominating fruitcrop in the region. This study area was used for area estimation of mango orchards from hyperspectral satellite data. EO-1-Hyperion image data of 13th April, 2005 with scene centre (Latitude- 29.17^0 and Longitude-77.7^0) has been used for the study.The scene characteristics of EO-1 Hyperion image of Meerut area are listed in the Table 1 below :

A field survey was conducted during 20th January, 2016 confined to Hyperion image coverage area of the Meerut to identify and locate major fruit crops grown in the region. Location co-ordinates were recorded using hand held Trimble GPS (June C). However, field survey revealed the major fruit crop over the site was only mango. During survey 24 mango orchard locations were identified as shown in black dots in Figure 1.a. on google image and green circles in the Hyperion image as shown in Fig. 1.b. Unique identification system was maintained for GPS locations and related fruit orchards throughout the study.

Before acreage estimation, hyperspectral satellite image need to be pre-processed followed by classification using SAM. Finally area was estimated using pixel counting method. The entire methodology for area estimation is explained with the help of flowchart in Fig. 2. and the detail steps for area estimation are elaborated below:

The pre-processing stage can be considered as the first stage to be undertaken to work with the hyperspectral data sets and to collect the valuable information from the data sets. Spaceborne hyperspectral data sets require careful pre-processing

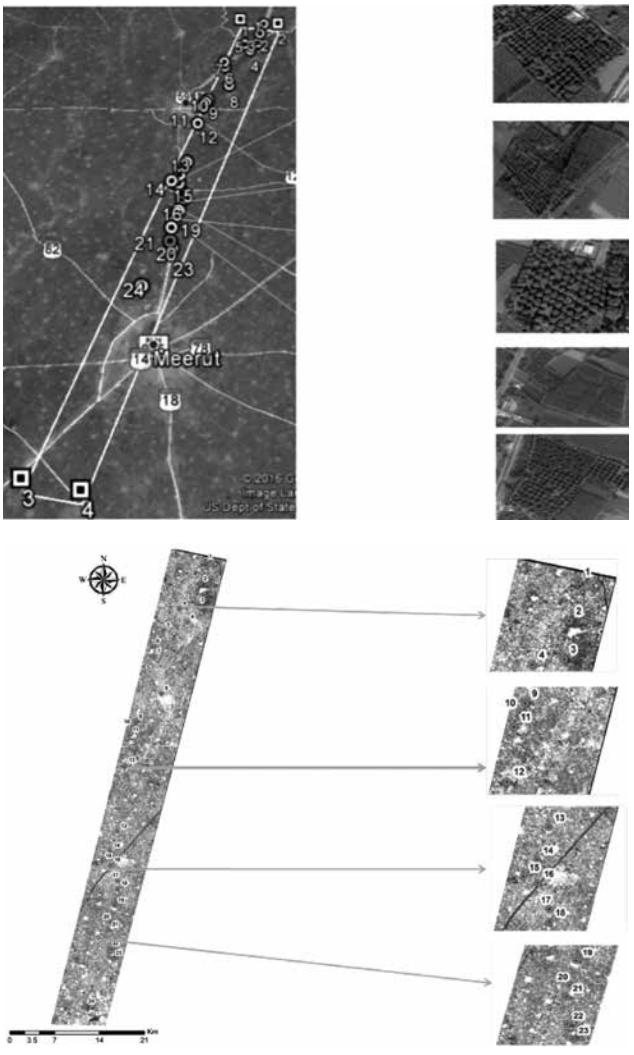

Fig. 1. Location of 24 mango orchards on (a) Google image and (b) Hyperion image of study area.

Table 1. Scene Characteristics of EO-1 Hyperion data of Meerut Area.
(Source: http://edcsns17.cr.usgs.gov/NewEarthExplorer)

Data attribute	Attribute value	Data attribute	Attribute value
entity ID	EO11460402005103110PF_PF1_01	Scene Start Time	2005_103_05:07:05
Acquisition Date	April 13, 2005	Scene Stop Time	2005_103_05:11:25
Site coordinates	29.17, 77.70	Date Entered	April 13, 2005
NW Corner	29.712443, 77.800198	Target Path	146
NE Corner	29.698625, 77.876903	Target Row	40
SW Corner	28.796505, 77.566649	Sun Azimuth	125.40
SE Corner	28.782861, 77.642726	Sun Elevation	59.03
Cloud Cover	0-9%	Satellite Inclination	98.21
Receiving Station	PF1	Look Angle	-2.1523

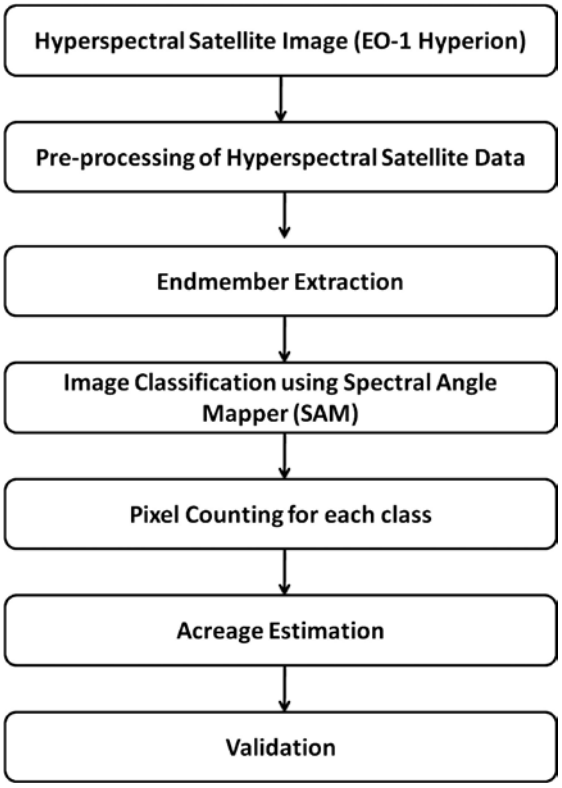

Fig. 2. Methodology for area estimation in mango.

because of their low spatial resolution which causes the mixing of spectral response of features within apixel. As hyperspectral sensors acquire data in narrow wavelength bands of width of the order of 10 nm, data volume is much more than the conventional system. Therefore, different pre-processing techniques applied to the data set in this work are bad band removal, image registration, atmospheric corrections, dimensionality reduction using Minimum Noise Fraction (MNF), purest pixel identification and extraction. Bad bands mean bands which do not provide any information should be removed. These are the water vapour absorption bands, overlapping bands, bands which are not illuminated properly. These bands should be removed because of higher noise level present in these bands. There are a number of corrupted pixels and dark vertical strips in the Hyperion datasets that are caused by calibration differences in the Hyperion detector array and temporal variations in the detectors response (Acito *et al*., 1). The geometric calibration of the image data can be done by the georeferencing. It is the simplest way of linking an image data to a projection system. Geometric correction is undertaken to avoid geometric distortions from a distorted image and is achieved by establishing the relationship between the image co-ordinate system and the geographic co-ordinate system using calibration data of the sensor, measured data of position, the ground control points, atmospheric conditions, etc. (Dobhal, 2). The electromagnetic signals recorded by the airborne or space borne hyperspectral sensors are a combination of the signals from earth's surface, atmospheric constituents and sensor errors. Thus, for quantitative analysis of the earth reflectance, these atmospheric effects need to be removed from the acquired signal and the procedure is called an atmospheric correction. The objective of atmospheric correction is to collect the surface reflectance (that characterises the surface features) from the hyperspectral imagery by removing the effects of atmosphere and it should be done carefully because it determines the usability of the final data. In atmospheric corrections, radiance values are converted into apparent surface reflectance, measuring the fraction of the radiation reflected from the earth surface. FLAASH module of ENVI is used for atmospheric correction of satellite images. In hyperspectral image processing, MNF is commonly used to align the data along the axis of decreasing

the signal to noise ratio (SNR). This technique is applied for removing redundancy and reducing dimensionality from hyperspectral data. It is a linear transformation consist of two separate PCA rotations in which at the first step it reduces the redundancy by creating independent bands which contain complete independent information and in the secondstep we select only first few transformed bands which may represent a very good percentage of information of original bands. The reflected spectrum of a pure feature is called a reference or *endmember* spectrum. Endmember spectra are extracted under idealized laboratory conditions where reflected spectrum is obtained with a spectrometer focused on a single feature. When this is impractical, the endmembers are derived from image manually. The Pixel Purity Index (PPI) is a commonly used algorithm for determining the purest pixels in an input image. The PPI algorithm ranks image pixels based on their pixel purity indices. Then, the pixels with the highest pixel purity values are returned as potential endmembers. The number of endmembers is not determined by this algorithm. It provides an interactive tool for extracting specific pure endmembers. Spectra can be thought of as points in n-dimensional scatter plot, where 'n' is the number of bands. Distribution of these points in n-space is used to estimate the number of spectral endmembers and their pure spectral signatures. It clusters the purest pixels and makes it separate class and then export the selected classes to ROIs and use them as input to classification.Based on the endmembers we classify the image by using Spectral Angle Mapper. SAM computes the spectral similarity betweenan image spectrum and the reference spectrum. If the angle is below a threshold angle (0.1 radian) then this classification procedure classify the pixel into endmembers class. The spectral angle mapper uses an n-dimensional angle to match pixels to reference spectra. The spectra of individual pixels are described as vectors in an n-dimensional space, where 'n' is the number of spectral bands. Each vector has certain length and direction. The length of the vector represents the brightness of the pixel while the direction represents the spectral feature of the pixel.To compare two spectra, such as an image pixel spectrum and a library reference spectrum, the multidimensional vectors are defined for each spectrum and the angle between the two vectors is calculated. Smaller angle means there is a close match to the reference spectrum. Spectral angle values are between 0 and $\pi/2$ and are calculated as

$$\theta = \cos^{-1}\left(\frac{\sum_{i=1}^{n} t_i r_i}{\sqrt{\sum_{i=1}^{n} t_i^2 \sum_{i=1}^{n} r_i^2}}\right) \quad (1)$$

where, n is the number of spectral bands, t is the reflectance of the actual spectrum and**r** is the reflectance of the reference spectrum.After the classification of EO-1 hyperion image of Meerut, total number of pixels in the mango orchards class wasidentified and then area of Mango orchards were obtained by multiplying the number of pixels classified into the mango class with the size of each pixel. Accuracy assessment of area estimation was done by using Google Earth.

RESULTS AND DISCUSSION

Hyperspectral satellite image contain huge volume of data which leads to redundancy and dimensionality problem. Therefore, before doing image classification different pre-processing techniques were applied to remove bad bands and atmospheric noise from the image and to reduce dimensionality in the data. In hyperspectral satellite image of Meerut, only 159 number of bands are found good and rest are bad bands. Those bad bands are removed from the data set before going to further pre-processing techniques (Fig. 3).

To select the Ground Control Point (GCP), permanent features like railway lines, road crossings, built up, etc. which are easy to locate on both map and Hyperion image is used. Root means square error (RMSE) for the geo-corrected image was found 0.43. Geo-correction also involves selection of the transformation projection and the Datum which was taken as Universal Transverse Mercator (UTM) and WGS84 respectively. Presence of atmospheric noise may influence the reflected radiation received by the sensor. So, atmospheric correction of EO-1 hyperion image of Meerut was done by using FLAASH module of ENVI (Fig. 4). In this module only basic information like site location, flight altitude, sensor model, local visibility and acquisition time required are needed

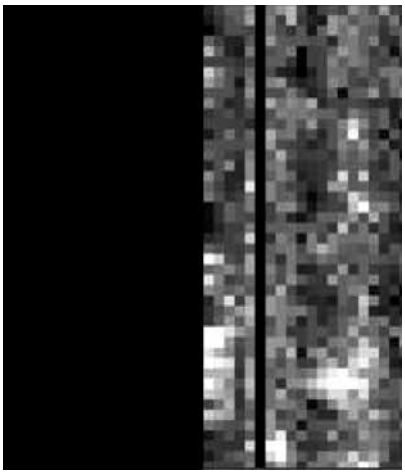

Fig. 3. Bad bands from EO-1 Hyperion image of Meerut.

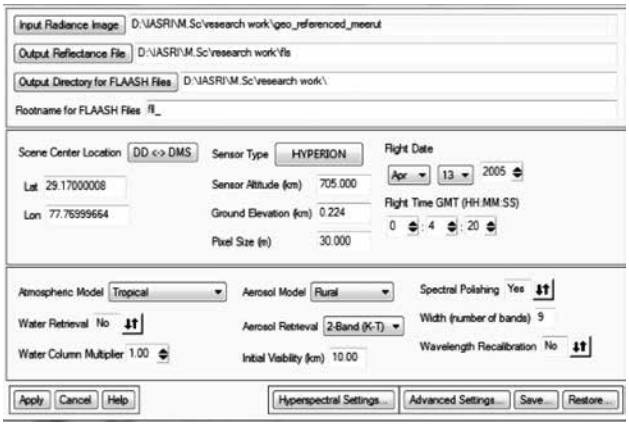

Fig. 4. FLAASH module for Atmospheric Correction.

to perform atmospheric correction. Fig. 5 shows the atmospherically corrected image.

On applying MNF on atmospherically corrected satellite image of Meerut, it was seen that only first 27 transformed bands contain almost 90% of the information of the original bands. Therefore, these 27 bands were selected for creating reduced MNF band image, which was later used for image classification. The MNF transformed image and MNF plot is shown in Fig. 6.

Endmembers were identified and extracted using PPI and n-Dimensional visualizer. This endmembers represent only mango orchards. In Fig. 7, PPI image and n-Dimensional visualizer window are shown. Based on the endmembers spectra of 24 Mango orchards image was classified using spectral angle mapper. The resulted SAM classified image is represented in Fig. 8.

Fig. 5. Atmospherically corrected image of Meerut.

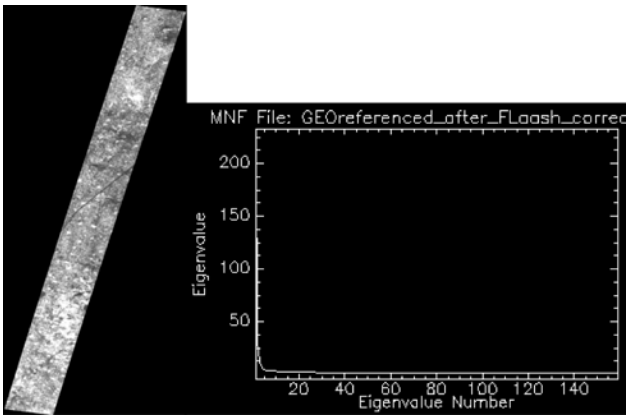

Fig. 6. MNF image and MNF plot of Hyperion image of Meerut.

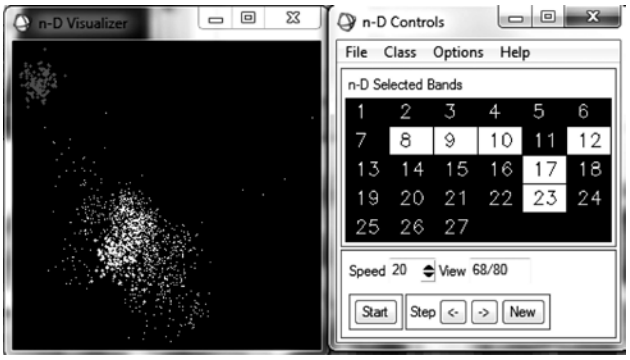

Fig. 7. PPI image and n-Dimensional plot of hyperion image.

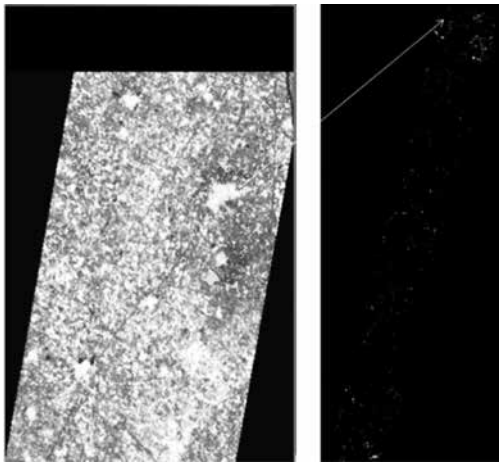

Fig. 8. SAM classified image.

After image classification, total number of pixels in the Mango orchard class were identified. Area of Mango orchards was obtained by multiplying the total number of pixels identified for mango orchard class with the size of each pixel. In the SAM classified image 9885 pixels of mango were identified. Since

the spatial resolution of the sensor is 30 m, the pixels size accounts to (30 × 30 sq. m.). Thus the total area under mango orchard is calculated as (9985 × 30 × 30 = 8896500) sq. meter or 889.65 hectare. Twenty four mango orchards were identified in the image (Paul, 5). The coordinates (latitude & longitude) of these mango orchards were recorded using GPS and are shown in Table 2.

Further, the area of 24 mango orchards was recorded using GPS and the area under these orchards was also obtained from the classified image which is shown in Table 3.

Further, regression analysis was performed assuming the actual area obtained from GPS as independent variable and area obtained using satellite data as dependent variable to predict the area under mango in the satellite image. The area obtained using satellite data was predicted using the constants of this regression equation. The plot of regression is shown in Fig. 9.

Table 2. Coordinates of mango orchards identified in the image.

Mango orchard No.	Mango orchard location	Latitude	Longitude
1	Before Gurukul Bus stop	29.696569°	77.848529°
2	Purquazi	29.665744°	77.841474°
3	BwPurquazi and Abdulpur	29.635641°	77.837343°
4	Mandla	29.612320°	77.823439°
5	Phalouda	29.631335°	77.812551°
6	Near Barla	29.600825°	77.789657°
7	Chhapar	29.578146°	77.775040°
8	Inside Chhapar-	29.563893°	77.776678°
9	Datiyana	29.512227°	77.787255°
10	Mustafabad	29.472328°	77.750959°
11	Mustafabad	29.465019°	77.747105°
12	Bilaspur	29.454020°	77.742200°
13	Salajuddi	29.411451°	77.736787°
14	Above Bhainsi	29.319025°	77.725439°
15	Nh58- Raipur Nagli	29.291349°	77.715821°
16	Phulat	29.277050°	77.704037°
17	Before Khatauli	29.271625°	77.716324°
18	Dhahbazpur Tingai	29.249603°	77.725881°
19	NH-58	29.238746°	77.726012°
20	NH-58	29.215010°	77.721677°
21	Sakoti Rly Stn	29.191875°	77.716030°
22	Near Sakoti	29.180903°	77.713486°
23	NH-58	29.154757°	77.713945°
24	Walidpur	29.140810°	77.718411°

Table 3. Comparison of area under GPS and Hyperion image.

Mango orchard No.	Area GPS (ha)	Area hyperion (ha)
1	3.22143	2.789
2	5.63895	4.891
3	3.85708	3.597
4	1.14708	1.049
5	4.42724	3.869
6	1.32623	0.912
7	1.65727	1.259
8	2.04305	1.987
9	3.08288	2.869
10	6.99187	5.997
11	2.03217	1.731
12	9.34408	8.036
13	0.37959	0.159
14	0.24720	0.259
15	0.30765	0.296
16	1.48500	1.289
17	1.14080	1.057
18	0.26256	0.055
19	0.69852	0.470
20	5.67319	4.865
21	1.36491	1.056
22	1.03190	1.023
23	23.15287	21.568
24	5.78992	4.978

The predicted area under the whole hyperion image was obtained as

$$Y = 1.081 \times (889.65) + 0.1726$$
$$= 961.71165 + 0.1726$$
$$= 961.88 \text{ ha}$$

A similar study was carried out by Panda et al., (7) In that study, fruit and nut crops were evaluated using many multispectral as well as one of the narrow band hyperspectral data and results of the study encouraged used of images for orchard mapping. The results of present study also endorse the use of satellite data for estimation of area under fruit crop. In hyperspectral satellite data, every pixel provides a reflectance spectrum that can be compared to the ground measured spectra. Therefore, the results of present investigation encourage the use of hyperspectral data to estimate acreage of orchards. The results of present study has quite good resemblance with the results of the study carried out by Taylor et al. (8). He also concluded that hyperspectral imagery offers

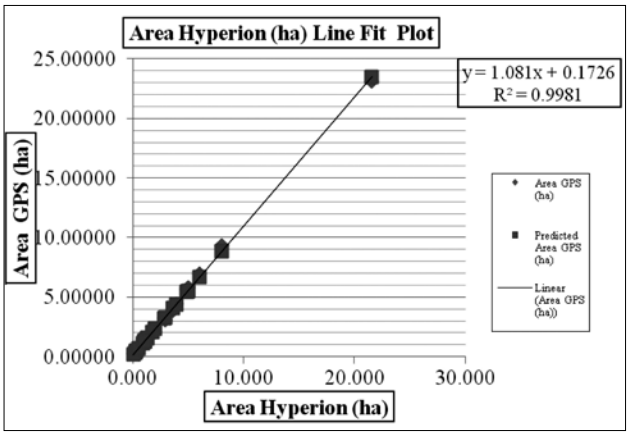

Fig. 9. Line of fit plot based on 24 Mango orchards (GPS points) of Meerut.

better estimation accuracy compared to multispectral imagery.

ACKNOWLEDGEMENT

The authors acknowledge the USGS-Earth Explorer (Source: https://earthexplorer.usgs.gov/). for providing free access to hyperspectral satellite data for this research work.

REFERENCES

1. Acito, N., Diani, M. and Corsini, G. 2010. Subspace-Based striping noise reduction in hyperspetral images. *IEEE Trans. Geosci. Remote Sens.* **49**: 1325-42.

2. Dobhal, S. 2008. Performance analysis of high-resolution and hyperspectral data fusion for classification and linear feature extraction. M.Sc. thesis, IIRS, Dehradun, India.

3. Gordon, D.K. and Philipson, W.D. 1986. Fruit tree inventory with Landsat thematic mapper data. *Photogram. Engg. Remote Sens.* **52Z**: 1871-76.

4. Nagaraja, A. 2010. Predicting susceptible areas of mango malformation through remote sensing and GIS, Ph.D. Thesis, IARI, New Delhi.

5. Paul, N.C. 2016. Statistical techniques for discrimination and acreage estimation of fruit crops using hyperspectral satellite data. M.Sc. thesis, P.G. School, Indian Agricultural Research Institute, New Delhi.

6. Yadav, I.S., Rao, N.K.S., Reddy, B.M.C., Rawal, R.D., Srinivasan, V.R., Sujatha, N.T., Bhattacharya, C., Rao, P.P.N., Ramesh, K.S., and Elango, S. 2002. Acreage and production estimation of mango orchards using Indian Remote Sensing (IRS) Satellite data. *Scientia Hort.* **93**: 105-23.

7. Panda, S.S., Hoogenboom G. and Paz J.O. 2010. Remote sensing and geospatial technological applications for site-specific management of fruit and nut crops: A review. *Remote Sens.* **2**: 1973-97.

8. Taylor, S., Kumar, L. and Reid, N. 2011. Comparison of broadband and hyperspectral sensors for Lantana mapping. ISPRS Archives 2011, pp. 1-4.

9. Schupp, J., Baugher, T., Travis, J., Hull, L., Ngugi, H., Krawczyk, G., Harsh, M., Reichard, K., Ellis, K., Remcheck, J., Crassweller, R., Marini, R., Harper, J., Kime, L., Heinemann, P., Liu, J., Lewis, K., Hoheisel, G., Jones, V., Glenn, M., Miller, S., Tabb, A., Park, J., Slaughter, D., Johnson, S., Landers, A., Reichard, G., Singh, S., Bergerman, M., Kantor, G., Messner, W. 2009. *Speciality Crop Innovations: Progress and Future Directions, Specialty Crop Innovations Progress Report*, College of Agricultural Sciences, Penn State University: University Park, PA, USA, pp. 1-16.

10. Tajeda, P.J.Z., Berjon, A., Miller, J.R. 2004. Stress detection in crops with hyperspectral remote sensing and physical simulation models. **In**: *Proceedings of Airborne Imaging Spectroscopy Workshop*, Bruges, Belgium, October 8.

11. Ye, X., Sakai, K., Garciano, L.O., Asada, S.I. and Sasao, A. 2006. Estimation of citrus yield from airborne hyperspectral images using a neural network. *Ecol. Model*. **198**: 426-32.

Received : July, 2017; Revised : December, 2017;
Accepted : February, 2018